YMTHE, Volume *32*

Supplemental Information

Prevention of prostate cancer metastasis by a CRISPR-delivering nanoplatform for interleukin-30 genome editing

Cristiano Fieni, Stefania Livia Ciummo, Carlo Sorrentino, Simona Marchetti, Simone Vespa, Paola Lanuti, Lavinia Vittoria Lotti, and Emma Di Carlo

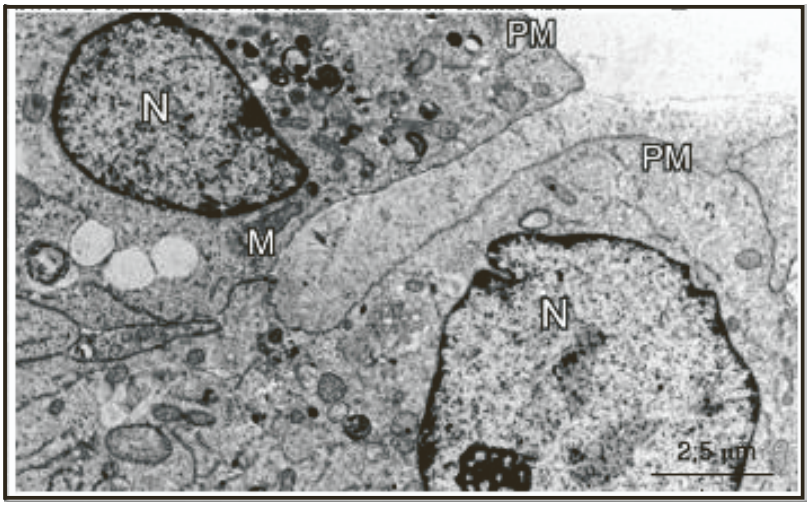

Figure S1. Ultrastructural features of untreated DU145 cells *in vitro*. DU145 cells, untreated or PBS-treated, did not exhibit the typical electron-dense spherical vesicles eitherin the extracellular or cytoplasmic sites. N, nuclei. M, mitochondria. PM, plasma membrane.Ultrastructural images of untreated PC3 cells also lacked the electron-dense spherical vesicles.

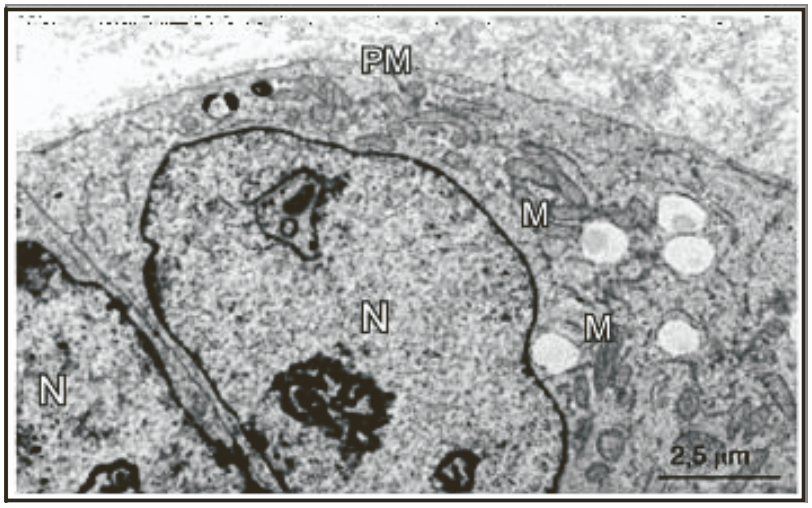

Figure S2. Ultrastructural features of untreated DU145 cells *in vivo*. DU145 cellclusters, lodged in the lungs of PBS treated mice, lacked the typical electron-dense sphericalvesicles either in the extracellular or cytoplasmic sites. N, nuclei. M, mitochondria. PM, plasma membrane. Ultrastructural images of PC3 cell clusters from the lung of PBS treatedmice, also lacked the electron-dense spherical vesicles.

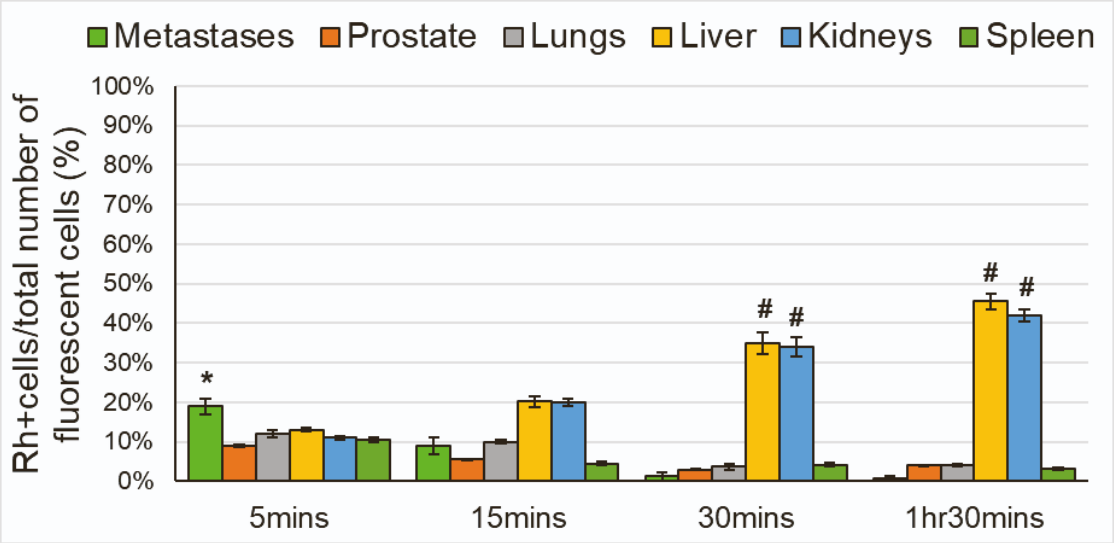

Figure S3. Quantification of the uptake of NPs by lung metastases, lung parenchyma, prostate, spleen, liver and kidneys, evaluated by LSC microscopy, in mice injected with wild-type DU145 cells and treated with RhB-NPs. NP uptake was assessed by LSC microscopy, using ZEN Microscopy Software. Results are expressed as mean percentage of RhB^+GFP^+cells/total number of GFP^+cells (for lung metastasis), of RhB^+EpCam^+cells/total number of $EpCam^+$cells (for lung parenchyma) and of $RhB^+Phalloidin^+$cells/total number of $Phalloidin^+$cells (for prostate, spleen, liver and kidneys). ANOVA: $p<0.001$. *$p<0.01$, Tukey HSD test versus organs at the same time point.$^{\#}p<0.01$, Tukey HSD test versus tumor and other organs at the same time point. The resultsare comparable with those obtained in mice injected with wild-type PC3 cells and treated with RhB-NPs.

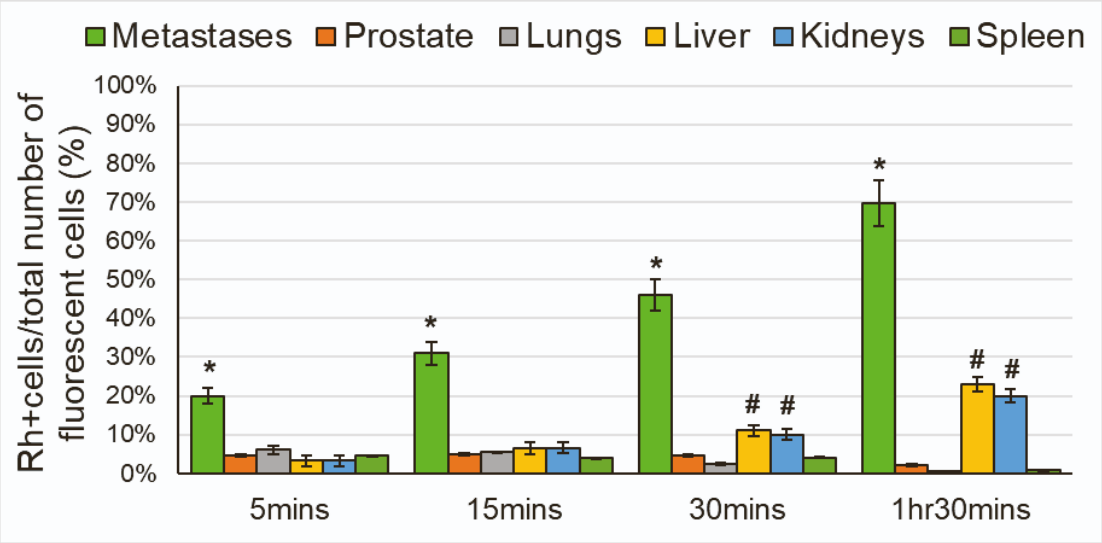

Figure S4. Quantification of the uptake of NPs by lung metastases, lung parenchyma, prostate, spleen, liver and kidneys, evaluated by LSC microscopy, in mice injected with wild-type DU145 cells and treated with RhB-PSCA-NPs. NP uptake was assessed by LSC microscopy, using ZEN Microscopy Software. Results are expressed as mean percentage of RhB^+GFP^+cells/total number of GFP^+cells (for lung metastasis), of RhB^+EpCam^+cells/total number of $EpCam^+$cells (for lung parenchyma) and of $RhB^+Phalloidin^+$cells/total number of $Phalloidin^+$cells (for prostate, spleen, liver and kidneys). ANOVA: $p<0.001$. *$p<0.01$, Tukey HSD test versus organs at the same time point. $^{\#}p<0.01$, Tukey HSD test versus other organs at the same time point. The results are comparable with those obtained in mice injected with wild-type PC3 cells and treated with RhB-PSCA-NPs.

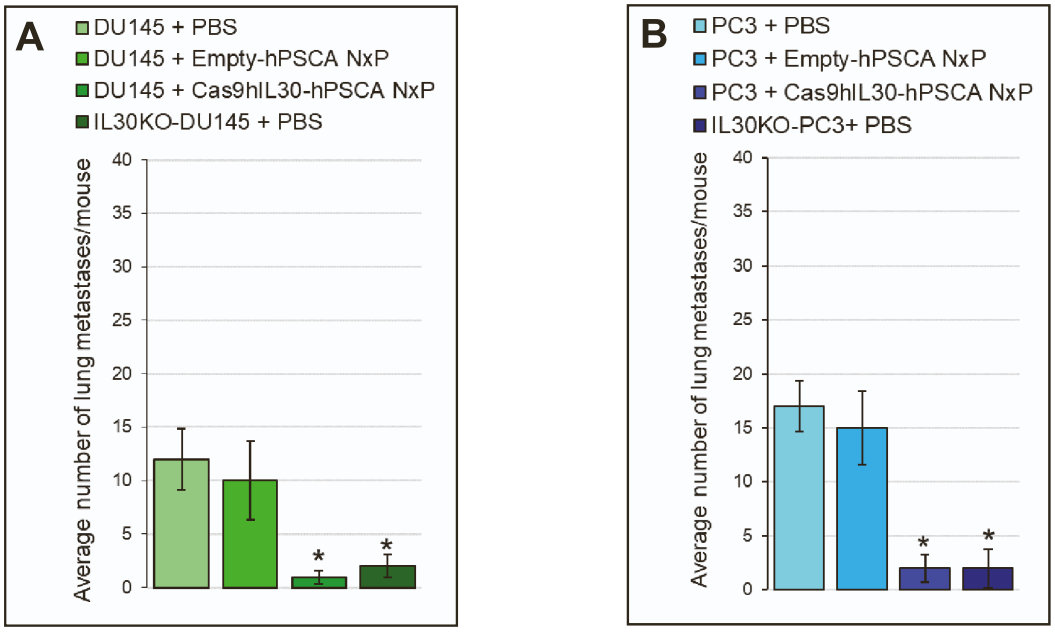

Figure S5. Treatment of lung PC microemboli with ImmunoLiposomes carrying Cas9gRNA-*hIL30*.

A. Mean number of lung metastasis developed in NSG mice, after i.v. injection of IL30KO or wild type DU145 cells, and 3 treatments with PBS, or Empty-PSCA NP, or Cas9*hIL30*-PSCA NP. ANOVA: $p<0.01$. *$p<0.01$, Tukey HSD test compared with DU145 tumor microemboli treated with PBS or Empty-PSCA NP.

B. Mean number of lung metastasis developed in NSG mice, after i.v. injection of IL30KO or wild type PC3 cells, and 3 treatments with PBS, or Empty-PSCA NP, or Cas9*hIL30*-PSCA NP. ANOVA: $p<0.0001$. *$p<0.01$, Tukey HSD test compared with PC3 tumor microemboli treated with PBS or Empty-PSCA NP. ANOVA: $p<0.001$. *$p<0.01$, Tukey HSD test compared with PC3 tumor microemboli treated with PBS or Empty-PSCA NP.

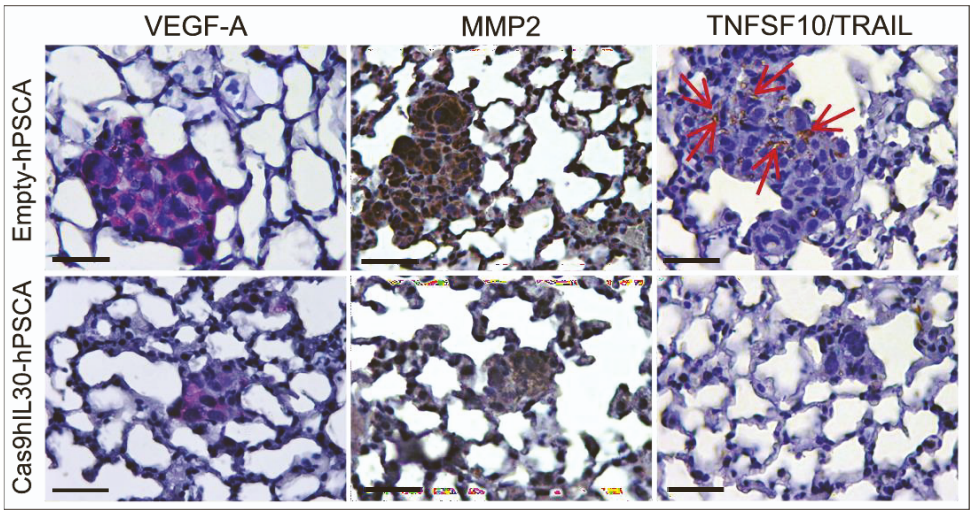

Figure S6. Immunopathological features of lung metastasis from ImmunoLiposome treated mice.

Lung metastasis, developed after i.v. inoculation of DU145 cells, from Empty-PSCA NP treated mice show a robust expression of VEGF-A (a), MMP2 (b) and faint cancer cell surface expression of TNFSF10/TRAIL (c). By contrast, metastasis developed in Cas9*hIL30*-PSCA NP-treated animals show a weak expression of VEGF-A (d), and MMP2 (e), while the expression of TNFSF10/TRAIL was absent (f). Immunopathological features of lungs from mice injected with wild type DU145 cells, and treated with PBS were comparable to those of lungs from Empty-PSCA treated mice. Results from mice bearing lung metastasis developed after i.v. inoculation of PC3 cells were comparable to those obtained from mice bearing lung metastasis developed after i.v. inoculation of DU145 cells. Magnification: X400. Scale bars: 40 μm.

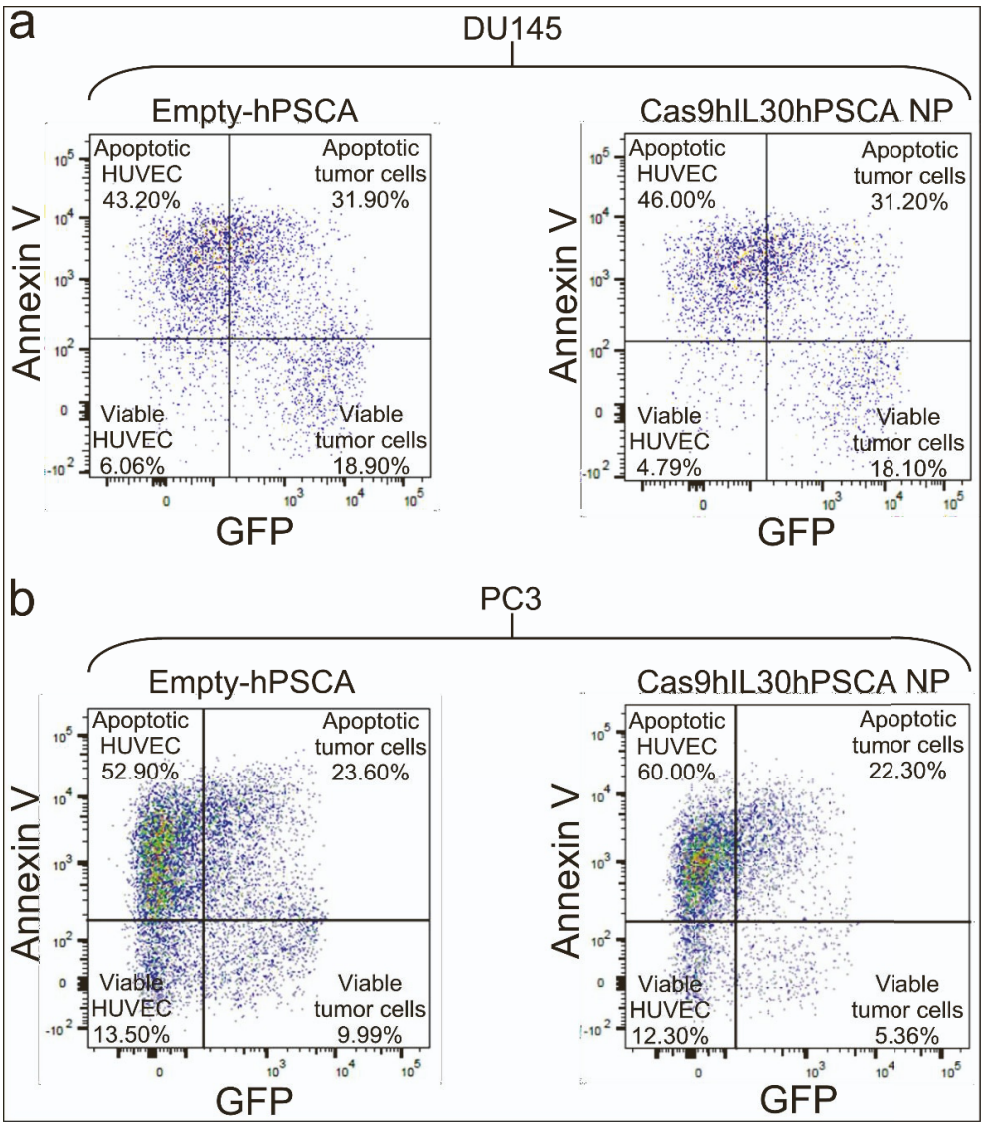

Figure S7. Annexin V assay on lung spheroids from the 2-OC after ImmunoLiposome treatments.

Flow cytometric analysis of apoptosis, by Annexin V assay, on DU145 cells + HUVEC (**a**) and PC3 cells + HUVEC (**b**) forming tumor spheroids in the PC-lung on a chip, after the treatment with 5 doses of ImmunoLiposomes. The image is representative of a triplicate experiment. $p>0.05$, Student's *t*-test between apoptotic and viable tumor cells and apoptotic and viable HUVEC.

Table S1. Particle size and zeta potential of Empty-PSCA and Cas9*hIL30*-PSCA NPs

NPs	Size (nm)	Zeta (mV)
Empty-PSCA NPs	75.8 ± 0.4	20.41 ± 3.16
Cas9 gRNA-*hIL30*-PSCA NPs	81.8 ± 0.5	5.05 ± 1.60

Table S2. Off-target sites, identified by whole-genome sequencing, associated with the TrueGuide sgRNA CRISPR947272_SGM and sgRNA 780 CRISPR947284_SGM, used for IL30 gene editing in DU145 and PC3 cells, respectively (**see the attached excel file "Table S2").**

Table S3. Levels of metabolic markers and inflammatory cytokines in serum samples from BALB/c mice treated with Cas9*hIL30*-PSCA NPs or PBS

	BALB/c	
	PBS	**Cas9*hIL30*-PSCA NPs†**
Metabolic markers*		
ALT	15.03 ± 3.23 IU/l	16.50 ± 2.63 IU/l
AST	24.32 ± 2.25 IU/l	25.98 ± 3.00 IU/l
BUN	21.22 ± 3.78 mg/dl	22.99 ± 5.50 mg/dl
CK	160.97 ± 11.73 u/l	167.51 ± 11.21 u/l
Cr	0.50 ± 0.11 mg/dl	0.55 ± 0.20 mg/dl
cTn1	37.30 ± 4.35 ng/ml	39.99 ± 5.00 ng/ml
LDH	275.32 ± 24 u/ml	287.23 ± 17.05 u/ml
Cytokines#		
IL6	95.22 ± 20.44 pg/ml	103.45 ± 20.63 pg/ml
TNFα	49.08 ± 19.17 pg/ml	52.10 ± 16.48 pg/ml

ALT, alanine aminotransferase; **AST**, aspartate aminotransferase; **BUN**, blood urea nitrogen; **CK**, creatine kinase; **Cr**, creatinine; **cTn1**, cardiac troponin-1; **IU/l**, international units per liter; **LDH**, lactate dehydrogenase; **u/l**, units per liter; **u/ml**, units per milliliter.
*****Levels measured 21 days after starting treatment.
#Levels measured 24 hrs after the first treatment.
†Results from mice treated with naked Cas9*hIL30* complex or Empty-PSCA NPs were comparable to those from mice treated with Cas9*hIL30*-PSCA NPs.

Table S4. Primers used for real-time RT-PCR

Gene	Product code or sequences	Source
Genes Regulators of EC activation, proliferation and sprouting		
ACKR1	QT00208719	Qiagen, Hilden, Germany
ACKR3	QT00069650	Qiagen
ANG	QT01675212	Qiagen
CCL2	QT00212730	Qiagen
CCR2	QT00000224	Qiagen
CTGF	QT00052899	Qiagen
CXCR2	QT00000518	Qiagen
CXCR4	QT00223188	Qiagen
DLL4	QT00081004	Qiagen
EDN1	QT00088235	Qiagen
FGF1	QT00079317	Qiagen
FGF2	QT00047579	Qiagen
IL8	Forward 5'-ATCTCACTGTGTGTGTAAACATGACTTCC-3' Reverse 5'-CACTGACATCTAAGTTCTTTAGCACTCC-3'	Merck, Burlington, MA, USA
JAG1	QT00031948	Qiagen
MMP14	QT00001533	Qiagen
MMP2	Forward 5'-AGCGAGTGGATGCCGCCTTTAA-3' Reverse 5'-CATTCCAGGCATCTGCGATGAG-3'	Thermo Fisher, Waltham, MA,USA
MMP9	Forward 5'-GCCACTACTGTGCCTTTGAGTC-3' Reverse 5'-CCCTCAGAGAATCGCCAGTACT-3'	"
PDGFA	QT01664488	Qiagen
TGFB1	QT00000728	Qiagen
VEGF-R1	QT00073640	Qiagen
VEGF-R2	QT00069818	Qiagen

Epithelial-to-mesenchymal transition (EMT) genes		
AKT1	Forward 5'-TGGACTACCTGCACTCGGAGAA-3' Reverse: 5'-GTGCCGCAAAAGGTCTTCATGG-3'	Thermo Fisher
BMP7	QT00068936	Qiagen
CDH1	QT00080143	Qiagen
ITGB1	QT00068124	Qiagen
MMP2	Forward 5'-AGCGAGTGGATGCCGCCTTTAA-3' Reverse 5'-CATTCCAGGCATCTGCGATGAG-3'	Sigma
MMP9	Forward 5'-GCCACTACTGTGCCTTTGAGTC-3' Reverse 5'-CCCTCAGAGAATCGCCAGTACT-3'	Merck
NOTCH1	QT00231056	Qiagen
SNAI1	Forward 5'-CCTCTTCCTCTCCATACCT-3' Reverse 5'-TTCATCAAAGTCCTGTGGG-3'	Merck
SNAI2	Forward 5'-TGTCATACCACAACCAGAGA-3' Reverse 5'-CTTGGAGGAGGTGTCAGAT-3'	"
STAT3	QT00068754	Qiagen
TGFB1	QT00000728	Qiagen
TWIST1	Forward 5'-CGGAGACCTAGATGTCATT-3' Reverse 5'-CTGTCTCGCTTTCTCTTTT-3'	Merck
TWIST2	Forward 5'-AACTGGACCAAGGCTCTC-3' Reverse 5'-GCGGCGTGAAAGTAAGAAT-3'	"
VIM1	QT00095795	Qiagen
WNT11	QT00018270	Qiagen
WNT3A	QT00220542	Qiagen
WNT5A	QT00025109	Qiagen
ZEB1	Forward 5'-CCAACAGACCAGACAGTG-3' Reverse 5'-TGACTCGCATTCATCATCTT-3'	Merck
ZEB2	Forward 5'-CGGAGACTTCAAGGTATAATC-3' Reverse 5'-GTTACGCCTCTTCTAATGACA-3'	"

Table S5. Antibodies used in immunostaining

Antibody	Clone	Origin	Research Resource Identifiers (RRIDs) or product code	Source
Anti-human				
CDH1	NCH-38	Mouse	RRID:AB_2076672	Agilent, Santa Clara, CA, USA
Ki67	MIB1	Mouse	RRID:AB_2142367	"
IGF1		Rabbit	RRID:AB_308724	Abcam, Cambridge, UK
IL30		Rabbit	RRID:AB_10898806	"
METAP-2		Mouse	RRID:AB_2723358	"
PSCA		Rabbit	RRID:AB_2662130	"
CXCL2	OTI1F6	Rabbit	500-P130	PeproTech EC, London, UK
MMP2		Mouse	RRID:AB_2881746	Proteintech, Rosemont, IL, USA
TNFSF10 (TRAIL)	2B10D1K18	Goat	SC-6079	Santa Cruz Biotechnology, Texas, USA
VEGF-A		Rabbit	RRID:AB_149827	Thermo Fisher, Waltham, MA,USA
Anti-mouse				
CD11b	EPR1344	Rabbit	RRID:AB_2650514	Abcam, Cambridge, UK
Gr-1	RB6-8C5	Rat	RRID:AB_394638	BD Biosciences, Franklin Lakes, NJ, USA
Ly-6G	1A8	Rat	RRID:AB_1089179	BioLegend, San Diego, CA, USA

SUPPLEMENTAL MATERIALS AND METHODS

Flow cytometry and antibody conjugation efficiency

To assess PSCA expression, DU145 and PC3 cells were harvested and mechanically dissociated into a single cell suspension. The cells were pelleted and resuspended in PBS with 0,5% BSA and incubated for 30 mins, at 4 °C, with anti-PSCA Ab (Thermo Fisher Scientific Cat# PA5-65080, RRID:AB_2662130). Subsequently, cells were pelleted and washed in PBS, and incubated for 30 mins, in at 4 °C, with Alexa fluor 488 secondary Ab (Thermo Fisher Scientific Cat# A-11008, RRID:AB_143165). Acquisition was performed using a BD Scientific Canto II Flow Cytometer (RRID:SCR_018056), and the data were analyzed using FlowJo software (RRID:SCR_008520). Dead cells were excluded by 7AAD staining.

Conjugation efficiency, between the anti-PSCA Ab and the Aldheyde-modified DSPE-PEG2000 lipid present on the external layer of the NP, was assessed by flow cytometry. Briefly, $1x10^6$ PC cells were seeded in T25 cell culture flasks and, after 24 hrs, they were incubated for 1 hr with Rhodamine labelled NPs, conjugated or not with anti-PSCA Abs. Cells were harvested and mechanically dissociated into a single cell suspension. The cells were then pelleted by centrifugation at 230g, washed in PBS, and analysed as described above.

TEM analyses of prostate cancer spheroids incorporated in the 2-OC platform

The 3D PC spheroid models, composed by DU145 or PC3 cells, and HUVEC, cocultured into a 24-well ultra-low attachment plate (#174930; Thermofisher Scientific) were treated with a 1:25 dilution of Cas9IL30 NPs, or Cas9IL30-PSCA NPs, for 1, 2 or 3 hrs in fresh culture medium, or left untreated. Then, PC spheroids were fixed in 2.5% glutaraldehyde, post-fixed in osmium tetroxide, and embedded in Epon 812. Ultrathin sections were stained with uranyl

acetate–lead citrate and analyzed with a Philips CM10 and a Fei-Philips Morgagni 268D transmission electron microscope (Philips, Eindhoven, NL).

Assessment of PC and endothelial cell viability in PC spheroids

Viability and apoptosis of tumor and endothelial cells, were assayed by flow cytometry. At the end of the experiment, the tumor spheroids were collected from the insert of the 24-well compartment of the 2-OC chip and centrifuged. Supernatants from the samples were collected and frozen for subsequent analysis. The collected spheroids were washed with PBS and dissociated into a single cell suspension with Accumax Cell Aggregate Dissociation Medium (#00-4666-56; Thermofisher Scientific). Each sample was divided into two parts, one half was used for the proliferation analysis while the other half was used for the apoptosis assay.

Proliferation was investigated by Ki67 staining. Briefly, pelleted cells were fixed and permeabilized with the BD Cytofix/Cytoperm™ Fixation/Permeabilization Kit (#554714; BD Biosciences, Franklin Lakes, NJ, USA) according to manufacturer's protocol. The cells were then resuspended in staining buffer and incubated for 30 mins, at 4 °C, with anti-Ki67 antibody (Thermo Fisher Scientific Cat# 17-5698-82, RRID:AB_2688057). To detect apoptosis, Pacific Blue™ Annexin V/SYTOX™ AADvanced™ Apoptosis kit was used (#A35136; Thermofisher Scientific) according to manufacturer's protocol. All samples were counterstained with DRAQ5™ Fluorescent Probe Solution to identify individual cells (#62251; Thermofisher Scientific). Samples were acquired on BD FACS Verse Flow Cytometer, and the data were analyzed using FlowJo software (RRID:SCR_008520).

Proliferation and Apoptosis analysis of both tumor and endothelial cells was performed by 1) identifying the DRAQ5 positive cells, 2) by discriminating, from the DRAQ5 positive population, the GFP positive cells (DU145 or PC3 tumor cells) and GFP negative cells

(endothelial cells), 3) identifying the Ki67 positive cells and AnnexinV positive cells present in both the GFP positive and negative populations.

Assessment of PC cell colonization of lung spheroids or bone marrow scaffolds in the 2-OC platform

To assess the effects of the NP treatment on the metastatization process, the number of tumor cells (GFP^+) within the bone marrow scaffold or lung spheroids was quantified by flow cytometry. Briefly, at the end of the experiment both the bone marrow scaffold and lung spheroids were processed to obtain a single cell suspension. Subsequently, the bone marrow scaffolds were washed several times with a solution of PBE (PBS without calcium and magnesium, containing 0,5M EDTA and 0,6% BSA). The scaffolds were then incubated in this solution for 15 mins at room temperature and then washed and incubated with TrypLE™ Express Enzyme (#12605010; Thermofisher Scientific) at room temperature, for another 15 mins Both PBE and Tryple solutions, containing the cell suspensions, were collected and centrifuged at 300g for 10 mins, to pellet the cells. The pelleted cells were then resuspended in PBS and stained with Vybrant™ DyeCycle™ Violet Stain (#V35003; Thermofisher Scientific), to discriminate nucleated cells from potential debris of the bone marrow scaffold. The lung spheroids were collected, washed with PBS, and dissociated into a single cell suspension with Accumax Cell Aggregate Dissociation Medium (#00-4666-56; Thermofisher Scientific). The cells were then pelleted and resuspended in PBS and counterstained with Vybrant™ DyeCycle™ Violet Stain (#V35003; Thermofisher Scientific), to identify individual cells.

The cell suspensions from either bone marrow and lung spheroids were then acquired and analyzed on a BD FACS Verse Flow Cytometer. The quantification was perfomed 1) by identifying the Vybrant Dye positive cells, 2) by discriminating, from the Vybrant Dye positive

populations, the GFP positive cells. The number of GFP positive events were expressed in events/uL.

PCR array and real-time RT-PCR

RNA extraction was performed by using the RNeasy Mini Kit (#74104; Qiagen, Hilden, Germany), and reverse-transcribed with the RT^2 First Strand Kit (#330401; Qiagen). PCR array analyses were run on a Qiagen Rotor Gene Q (RRID:SCR_018976), using the RT^2 Profiler PCR Array Human Tumor Metastasis (#PAHS-028Z; Qiagen, Hilden, Germany). The results from each plate were normalized to the median value of a set of housekeeping genes. Changes in the gene expression were calculated using the ΔΔCt method. Results from experiments performed in triplicate were pooled and analyzed with the manufacturer's software. A significant threshold of a 2-fold change in gene expression corresponded to a $p<0.001$.

For the analysis of the expression of epithelial to mesenchymal (EMT) transition genes and genes involved in endothelial cells activation, proliferation and sprouting, the real-time RT-PCR reaction was performed with the Quantifast SYBR Green PCR Kit (#204054; Qiagen) and a MiniOpticon System (#CFB-3120; Bio-Rad, Hercules, CA, USA) using the primers listed in Table S4.

The results from each plate were normalized to the median value of the housekeeping gene HPRT. Changes in the gene expression were calculated using the ΔΔCt method. Results from experiments performed in triplicate were pooled and analyzed with the manufacturer's software. A significant threshold of a 2-fold change in gene expression corresponded to a $p<0.001$.

Histology, immunohistochemistry and TUNEL assay

For histology, tissue samples were fixed in 4%-formalin, embedded in paraffin, sectioned at 4-µm and stained with H&E. Single or double (CD11b/Gr-1, and NKp46/RORγt) immunostainings, on formalin fixed and paraffin-embedded, or frozen, tissue sections, were-performed as described,[1,2] by using the antibodies listed in the Table S5. Proliferation index and microvessel count were assessed by light microscopy, at ×400 in an 85,431.59 μm^2 field, on single immunostained sections, using QWin image analysis software (Leica QWin, RRID:SCR_018940), which ensures the following highly reproducible steps: 1) image acquisition; 2) conversion of RGB image (true colors) to binary image (black and white); 3) filtering to remove noise; 4) counting of immunostained cells or measurement of positively stained area. Six to eight high-power fields were analyzed for each section and three sections per sample were evaluated. The histopathological evaluation was performed excluding necrotic areas. Proliferation index was expressed as mean percentage ± SD of Ki67 positive cells/number of total cells per field (85431.59 μm^2). Microvessels were identified as small tubes or circles marked by CD31 Abs and results were expressed as mean ± SD of positive vessels/field. Immunostained sections were examined by two pathologists in a blind fashion, with very good agreement (κ value=0.89, 0.80 and 0.85, for evaluation of proliferation, apoptotic index, and microvessel density, respectively).

The assessment of granulocyte (Ly-6G) and myeloid-derived cell (Gr-1/CD11b) infiltrates of metastatic foci was performed according to the Tumor Area Positivity (TAP) score, as described in ref. doi: 10.1186/s13000-023-01318-8, using the QWin image analysis software (Leica QWin, RRID:SCR_018940) on single immunostained sections. Briefly, on each slide, the total area of metastases (tumor area) was visually identified by a pathologist and measured by the Qwin software. Subsequently, the $Ly6G^+$ granulocytes and $Gr\text{-}1^+/CD11b^+$ myeloid-derived cells infiltrating the tumor area were automatically counted by the Qwin software and the TAP score was obtained using the following formula: area covered by Gr-

1^+, or Gr-1^+/$CD11b^+$ cells/total tumor area x 100. Three sections per sample were evaluated by two pathologists in a blind fashion, with very good agreement (κ value=0.89).

The human prostate tissue samples, for immunostaining with anti-PSCA Abs, were obtained from the institutional Biobank of the Local Health Authority n. 2 Lanciano - Vasto - Chieti (Italy) and the personal data processing complies with Data Protection Laws.

REFERENCES

1. Sorrentino C, D'Antonio L, Ciummo SL, Fieni C, Landuzzi L, Ruzzi F, Vespa S, Lanuti P, Lotti LV, Lollini PL, et al. CRISPR/Cas9-mediated deletion of Interleukin-30 suppresses IGF1 and CXCL5 and boosts SOCS3 reducing prostate cancer growth and mortality. J Hematol Oncol. 2022 Oct 13;15(1):145.
2. Sorrentino C, Ciummo SL, D'Antonio L, Fieni C, Lanuti P, Turdo A, Todaro M, Di Carlo E. Interleukin-30 feeds breast cancer stem cells via CXCL10 and IL23 autocrine loops and shapes immune contexture and host outcome. J Immunother Cancer. 2021 Oct;9(10):e002966.